Energy Technology
Generation, Conversion, Storage, Distribution
www.entechnol.de

Fabrication of Self-Cleaning CNT-Based Near-Perfect Solar Absorber Coating for Non-Evacuated Concentrated Solar Power Applications

Raj Kumar Bera, Yaniv Binyamin, Cathy Frantz, Ralf Uhlig, Shlomo Magdassi, and Daniel Mandler**

A near-perfect black solar absorber made of carbon nanotubes (CNTs) prepared by a low-cost wet-deposition method on a reflective metal surface for mid-temperature non-evacuated concentrated solar power (CSP) applications is demonstrated. The dispersed CNTs in an alumina–silica matrix exhibit an absorptance of 0.985 in the entire solar spectrum and emittance of 0.90 in the infrared (IR) region. The coating shows high durability and is super-hydrophilic (0° contact angle) after plasma treatment, without affecting the solar absorptance and excellent coating adhesion. The efficiency of the coating is evaluated by analytical models, which implies that it has higher efficiency at low temperature and at a high solar concentration ratio than that of previously reported selective coatings.

1. Introduction

An ideal blackbody absorbs all incident electromagnetic radiation, regardless of frequency or angle of incidence, and therefore, the absorptance of such blackbody is 1.[1] In reality, such a blackbody does not exist. Therefore, an object which has an absorptance in the range of 0.98–0.99 is called near-perfect blackbody absorber.[1–5] The near-perfect blackbody absorbers have several applications, such as stray light shielding, optical detectors, radiometers in space-borne infrared (IR) systems, solar cells, and absorbers in concentrated solar power (CSP) systems.[1–14] The overall efficiency of CSP systems with a large concentration factor of the solar flux is nearly proportional to its absorptance of the solar spectrum.[15] As a rule of thumb, a decrease of 10% in emittance is equivalent to an increase of 1% in absorptance at high concentration ratios.[16] Hence, in CSP systems, increasing the value of solar absorptance is more significant than reducing the IR emittance.[15]

CNT is the best absorbing material ever produced as stated by NASA.[17] Because of their unique optical property and their high thermal conductivity, CNTs are excellent candidates for solar absorber coatings. Recently, several groups have reported the fabrication of near-perfect blackbody absorbers with vertically-aligned CNT forests by chemical vapor deposition (CVD), having absorptance in the range of 0.98–0.99.[1–5,10,11] Vertically -aligned CNT films were reported by Mizuno et al. having an absorptance of 0.98–0.99 at 0.2–200 μm[1] and by Yang et al. who demonstrated extremely high absorptance of ≈99.9% in the range of 457–633 nm.[4] Selvakumar et al. reported the fabrication of a near-perfect blackbody absorber with an absorptance of 0.98–0.99 using a 10 μm-thick CNT tandem absorber fabricated by CVD.[5] Similarly, Cao et al. constructed a tandem structure by CVD with aligned CNTs on a quartz sheet with an absorptance of 0.98.[10] Kaul et al. formed vertically-aligned CNT ensembles on a metallic substrate, which exhibited a very low reflectance of 0.02%.[11] The high absorptance of CNT forests results from the low-effective refractive index, which is due to the low material packing density.[5] Although the near-perfect absorber can be fabricated by CVD, this involves high temperatures, special catalysts, flammable gases (hydrogen), and costly equipment.

For CVD-fabricated CNT forests, little attention has been given to the adhesion of the CNTs to the substrate and their stability at high temperatures in air. It is well known that the adhesion of CNTs (including vertically grown) to metallic surfaces is poor since there is no binder or matrix to bind the CNTs tightly to the substrate. Therefore, it is greatly desired to develop rapid and simple wet-deposition processes for the fabrication of highly absorbing CNT-based black coatings with excellent adhesion and high thermal stability. This is achievable by incorporating the CNTs within a heat-resistant matrix, which has excellent adhesion to the surface. However, previous reports revealed that CNT coatings fabricated by wet-chemical methods resulted in lower absorptance as compared with CVD processes.[18–24] Rincon et al. fabricated TiO_2/CNT tandem absorbing coating by the sol-gel process, yielding low solar absorptance.[18] Roro et al. reported on nanocomposite coatings composed of multiwalled carbon nanotubes (MWCNTs) and

Dr. R. K. Bera, Y. Binyamin, Prof. S. Magdassi, Prof. D. Mandler
Institute of Chemistry
The Hebrew University of Jerusalem
Jerusalem 9190401, Israel
E-mail: magdassi@mail.huji.ac.il; daniel.mandler@mail.huji.ac.il

Dr. C. Frantz, Dr. R. Uhlig
Institute of Solar Research
German Aerospace Center
Pfaffenwaldring 38-40, Stuttgart 70567, Germany

The ORCID identification number(s) for the author(s) of this article can be found under https://doi.org/10.1002/ente.202000699.

DOI: 10.1002/ente.202000699

nickel oxide precursor by dip-coating, resulting in low absorptance of 0.84.[19] A solar absorbing coating was prepared with CNTs and alumina nanoparticles by electrophoretic deposition.[20] The resulting coating displayed an absorptance of only 0.7. The low absorptance of these coatings was probably due to the low thickness and density of the CNT film as well as the low absorptance of metal oxide in the NIR region. Kurzböck et al. prepared solar absorbers using CNT–polypropylene without metal oxide and achieved an absorptance of 0.94–0.95.[21]

Recently, we reported the wet-deposition coating of CNTs embedded in a polysiloxane matrix with an absorptance of 0.94–0.96.[22,23] The absorptance was further improved to 0.975 on adding a top coating of an anti-reflecting layer.[24] The simplicity of the wet-deposition method and the requirement of low-cost equipment make this approach superior to the reported CVD process for the fabrication of near-perfect solar absorbers.

Non-evacuated thermo-solar parabolic trough absorbers can be an attractive alternative to traditional evacuated parabolic troughs, because of their lower costs. However, they operate in the open air, under environmental conditions, which may cause oxidation and the accumulation of pollutants, thus, further decreasing their efficiency. For this reason, coatings with self-cleaning properties are highly desirable. It is well known that super-hydrophilic surfaces, with close to zero contact angle, exhibit self-cleaning properties as it enables simple removal of dirt from the surface by washing with water and imparts anti-fogging properties.[25,26] The wettability nature of the surface is affected by surface charge and roughness as well as by functional groups.[27] It was reported earlier that the plasma treatment can convert hydrophobic CNT surfaces to super-hydrophilic.[28,29]

Herein, we describe a simple, wet-deposition process (**Figure 1**) carried out at room temperature for the fabrication of near-perfect solar absorber with an absorptance of 0.985. Furthermore, a post-treatment by plasma results in a super-hydrophilic coating without affecting the absorptance. This coating shows excellent adhesion and is stable at 350 °C for >100 h with a constant water contact angle of 0°. Finally, analytical models reveal a higher absorber efficiency of the nonselective coating at low temperatures and high solar concentration ratio as compared with that of selective coatings.

2. Experimental Section

2.1. Materials

Multiwalled carbon nanotubes (MWCNTs, Baytubes cp70) were purchased from Bayer Material Science, AlOOH (Disperal P3) was from SASOL, Solsperse 46 000 from Lubrizol, and Byk 333 was from Byk-Chemie GmbH. Propylene glycol and methyltrimethoxysilane were purchased from Sigma-Aldrich.

2.2. Instrumentation

Reflectance spectra were recorded using CARY 5000 UV-visible-NIR spectrophotometer with an integrated sphere and the absorptance of the coatings were evaluated from the UV-vis-NIR reflectance spectra in the wavelength range of 0.3–2.5 μm using the equation, $\alpha + R + T = 1$, where α is absorptance, R is reflectance, and T is transmittance. Since the coatings were deposited on an aluminum substrate, the transmittance is zero, and therefore $\alpha = 1 - R$. The emittance was directly measured at room temperature using an Emissometer AE1/RD1 (Devices & Services Co, Dallas, Texas, USA) in the wavelengths range of 2–50 μm. Scanning electron microscopy (SEM) images were acquired using extra high-resolution SEM Magellan 400. The thickness of the coatings was measured with micro-TRI-gloss μ. For compositional analysis, energy dispersive X-ray spectroscopy (EDX) measurements were performed. XRD measurements were carried out with D8 Advance diffractometer (Bruker AXS, Karlsruhe) equipped with Göbel Mirror parallel-beam optics with Cu Kα radiation ($\lambda = 1.54$ Å).

2.3. Dispersion of CNT

A total of 0.24 g of carbon nanotubes (CNTs, Baytubes cp70), 0.12 g of dispersing agent (Solsphere 46 000), and 4.0 g of propylene glycol were mixed with 15.64 g distilled water. The mixture was sonicated for 7.5 min at 750 W in pulses of 1 s on and 1 s off with an amplitude of 85%.

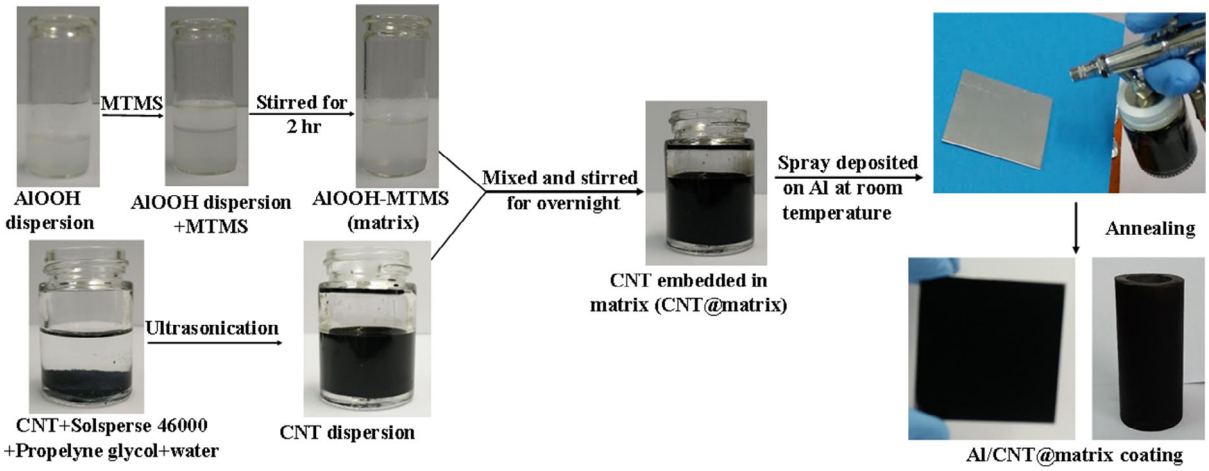

Figure 1. Schematic presentation of the CNT@matrix coating process.

2.4. Preparation of the Binder Solution

A total of 1.0 g of methyltrimethoxysilane was added to 2.0 g of an aqueous solution containing 10% AlOOH and stirred for 2.5 h.

2.5. CNT@matrix Coating

Five coating formulations were prepared by mixing 8.33, 6.66, 5.00, 3.33, and 1.66 g of the CNT dispersion and water to a final weight of 8.65 g. To this, 0.1 g of wetting agent (Byk 333) and 1.25 g of binder solution were added to form a final weight of 10 g. The final weight concentrations of the CNTs in the coating formulations were 1%, 0.8%, 0.6%, 0.4%, and 0.2%. The resulting mixture was stirred for 24 h and was sprayed (2.5 mL) on a $5 \times 5\,cm^2$ Al substrate at room temperature. The coated substrates were initially heated to 100 °C at a heating rate of $5\,°C\,min^{-1}$ for 30 min followed by heating to 350 °C at $10\,°C\,min^{-1}$ for 30 min. Finally, they were heated to 400 °C at a heating rate of $10\,°C\,min^{-1}$ for 60 min. A reference coating without the binder was prepared by spraying 2.5 mL of CNT dispersion onto a heated Al substrate (80 °C) followed by the same heat treatment. A schematic presentation of the steps involved in the formation of CNT@matrix coating is shown in Figure 1.

2.6. Plasma Treatment

After the heat treatment, the CNT@matrix coatings were treated with O_2 plasma by a low-pressure plasma chamber (Diener, PICO UHP, 40 kHz/200 W/0.2 mbar). The plasma parameters were: O_2, flow rate: $2\,cm^3\,min^{-1}$, plasma power: 200 w, and plasma duration: 5 min.

2.7. Adhesion Test

Adhesion test was performed according to standards ASTM D3359 and ISO 2409[27] using a cross-cut tester (Elcometer 1542 Cross Hatch Adhesion Tester). In this test, a lattice pattern was cut into the coating penetrating through the substrate. A tape was then placed on the cut pattern and pealed. The coating area was observed and the adhesion was rated in accordance with a standard scale.

2.8. Efficiency Evaluation in CSP Plants

An analytical model was used to evaluate the optical performance of the CNT@matrix coatings under the same conditions of a CSP plant and compared with two other selective coatings: W–Ni–Al_2O_3 cermet[30] and CNT/ITO inverse tandem.[23] The method was based on the concept of the selective absorber efficiency, η_{sel}, first proposed by Ho et al.[31]

$$\eta_{sel} = \frac{\dot{Q}_{rad,abs} - \dot{Q}_{rad,emit}}{\dot{Q}_{sol,inc}} \quad (1)$$

where $\dot{Q}_{rad,abs}$, $\dot{Q}_{rad,emit}$, and $\dot{Q}_{sol,inc}$ are the solar power absorbed, emitted, and incident per m of the absorber tube, respectively. The concept of η_{sel} was developed for tower receivers, assuming that the solar irradiated surface equals the radiating surface.

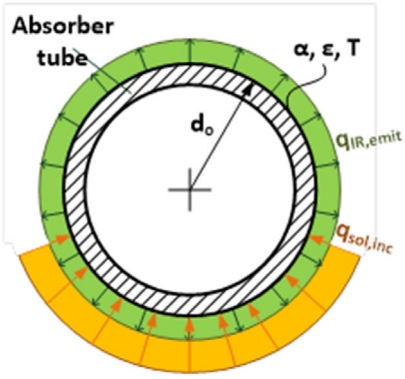

Figure 2. Schematic presentation of the three heat flows.

However, the CNT@matrix coatings presented in this study were intended for use in nonevacuated parabolic trough or Fresnel systems. In these systems, the solar irradiated surface represents ≈40% of the total tube surface, therefore, the following modified definition of the three heat flows was used (**Figure 2**).

$$\dot{Q}_{rad,abs} = \dot{q}_{sol,inc} \cdot a_{rad} \cdot \alpha_{sol} = CR \cdot \dot{q}_{DNI} \cdot a_{rad} \cdot \alpha_{sol} = \alpha_{sol} \cdot \dot{Q}_{sol,inc} \quad (2)$$

$$\dot{Q}_{rad,emit} = \varepsilon_{IR} \cdot \sigma \cdot a_{tot} \cdot T^4 \quad (3)$$

$$\dot{Q}_{sol,inc} = \dot{q}_{sol,inc} \cdot a_{rad} = CR \cdot \dot{q}_{DNI} \cdot a_{rad} \quad (4)$$

With:

$$a_{rad} = F_{rad} \cdot a_{tot} \quad (5)$$

$$a_{tot} = \pi \cdot d_o \quad (6)$$

F_{rad} is the fraction of the irradiated tube, d_o is the tube outer diameter, a_{tot} is the total, and a_{rad} is the solar irradiated circumference of the absorber tube. $\dot{q}_{DNI}$ is the global direct irradiation and CR is the concentration ratio from the concentrator. The solar absorptance α_{sol} and the thermal emittance ε_{IR} are computed based on measurement data of the spectral hemispherical absorptance, the solar emission ASTM G173-03 reference spectrum (AM 1.5), and the Planck function at absorber surface temperature T, respectively. Furthermore, the model assumes a constant irradiance over the irradiated circumference and constant absorber surface temperature. All further assumptions for each coating are listed in **Table 1**.

Table 1. The parameters of various coatings used in the simulation.

Parameters	CNT@matrix	W–Ni–Al_2O_3 cermet	CNT/ITO
Solar absorptance	0.985	0.900	0.938
Thermal emittance	0.901	0.150	0.270
Tube outer diameter [m]	0.042	0.042	0.042
Portion of irradiated area	0.4	0.4	0.4
Temperature [°C]	100, 250	100, 250	100, 250
Concentration ratio	30–230	30–230	30–230

3. Results and Discussion

The coating of CNT@matrix involves spraying of a dispersion of CNTs, Disperal P3, and methyltrimetoxysilane (MTMS) on an Al surface. Upon heating, as described above, this composition was converted into a heat-stable matrix. **Figure 3** shows the reflectance spectra and their corresponding images of a bare Al surface, and after coating with CNT only, the matrix composition, and with all the components. It can be seen that the reflectance of bare Al and Al coated with only the matrix components is high, whereas Al coated with only CNT and with CNT embedded in a matrix (CNT@matrix) shows substantially lower reflectance. The coating made by CNT only shows low reflectance of 3.6%, while that made by CNT embedded in the matrix shows even lower reflectance of ≈1.5% in the entire solar spectrum. This is in accordance with the visual image (Figure 3, top panel) whereby the substrate coated by CNT@matrix exhibits the darkest surface. The absorptance of the coatings was calculated from the UV-vis-NIR reflectance spectra and is presented in **Table 2**. The higher absorptance of CNT@matrix (0.985) than that of CNT only (0.964) may be due to multiple reflections between CNT and AlOOH.[32,33] The emissivity of the CNT@matrix coating was high, ≈0.90.

Figure 4 shows the dependence of the absorptance of the CNT@matrix on the CNT concentration in the matrix. It can be clearly seen that the absorptance of the coating increases with the increase of the concentration of CNT in the matrix.

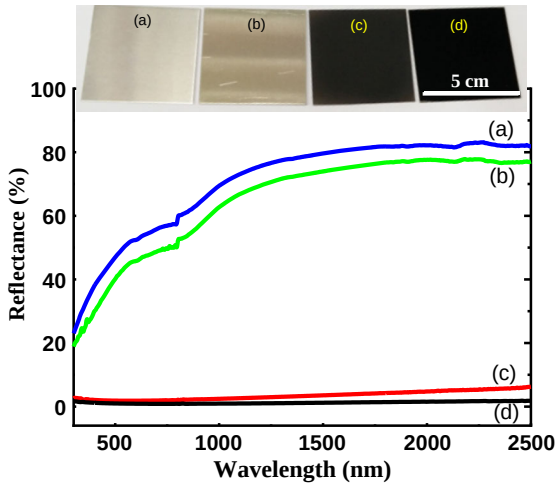

Figure 3. Reflectance spectra of different surfaces: a) Al substrate, b) Al substrate coated with matrix (Alumina + TMMS), c) Al substrate coated with only CNT, and d) Al substrate coated with CNT embedded in matrix. The upper panel shows photos of the corresponding coated surfaces.

Table 2. The absorptance value of different coatings.

Surface	Absorptance
Al	0.29 ± 0.001
Al/matrix	0.35 ± 0.001
Al/CNT	0.964 ± 0.002
Al/CNT@matrix	0.985 ± 0.002

The increase in absorptance is due to the close matches of the refractive index of CNT (1–1.8) with silica (1.4–1.55) and alumina (1.66) by which the matrix was prepared. At a concentration of 0.6% of CNT, the absorptance reaches 0.985 and levels off. To the best of our knowledge, this is the highest absorptance of a coating prepared by a wet-chemical method reported thus far (Table S1, Supporting Information). At low concentrations of CNT (0.2–0.4%) the lower absorptance is due to the contribution of the high reflectance of the Al. At higher CNT concentration (1%), the slightly lower absorptance may be due to the high electron density and permittivity of dense CNT, leading to an increase in the refractive index as the permittivity is proportional to the square of the refractive index.[5] At a CNT concentration of 0.6%, the high absorptance results from the low refractive index, 1.27, as calculated from the reflectance spectra using Fresnel's equation, because of the low material packing density.[1,5]

The adhesion of the solar-thermal coatings to the receiver substrate is an important parameter, which affects the lifetime of the receiver. Low adhesion leads to degradation of the coating over time, and therefore, requires a regular re-coating, which can be costly. Hence, an adhesion test was performed on the CNT coatings. It was found (**Figure 5**) that the adhesion of the CNT@matrix coating was very good (85–95%) and the Scotch tape did not remove the coating. By this adhesion test, ≈5–15% of the coating flaked along the edges and/or at the intersection of the cuts.[34]

Figure 6 shows the SEM images of CNT@matrix surface with 0.2%, 0.6%, 0.8%, and 1% of CNT in the coating dispersion. Evidently, in all the coatings, the CNTs are embedded in the matrix and the packing density increases with the increase in the concentration of the CNTs in the formulation. From the magnified SEM image (Figure 6f) it can be seen that the average diameter of CNTs is ≈30 nm and their walls are decorated with AlOOH particles. The cross sections of the coatings made of different CNT concentrations are measured in backscattering mode and are shown in Figure S1, Supporting Information. The thickness varies from 2.5 to 7 μm with increasing concentration of the CNT from 0.2% to 1% in the formulation. The bright spots in the images are the cross section of individual CNT (because of the high conductivity of CNT, the cross section appears as bright), showing that the density of CNT increases with the increase of the concentration of CNT in the formulation. The EDS analysis (Figure S2, Supporting Information) shows, as expected, the presence of C, Al, Si, and O. The XRD measurement of the coating shows the diffraction peak at $2\theta = 25^\circ$ corresponding to (002) plane of CNT (Figure S3, Supporting Information).

To impart self-cleaning properties to the coating, we modified the surface to make it super-hydrophilic. This was accomplished by oxygen plasma treatment, which caused a change in the contact angle of the surface from 90° to 0° (**Figure 7**). The as-prepared CNT coating exhibits high hydrophobicity due to the hydrophobic nature of CNT, whereas the oxygen plasma treatment generated oxygen functionalities (as confirmed by XPS spectra, Figure S4, Supporting Information), which significantly increased the wettability of the surface and therefore, decreased significantly the contact angle. The 0° contact angle and the porous structure of the coating resulted in a super-hydrophilic surface. To further evaluate the self-cleaning

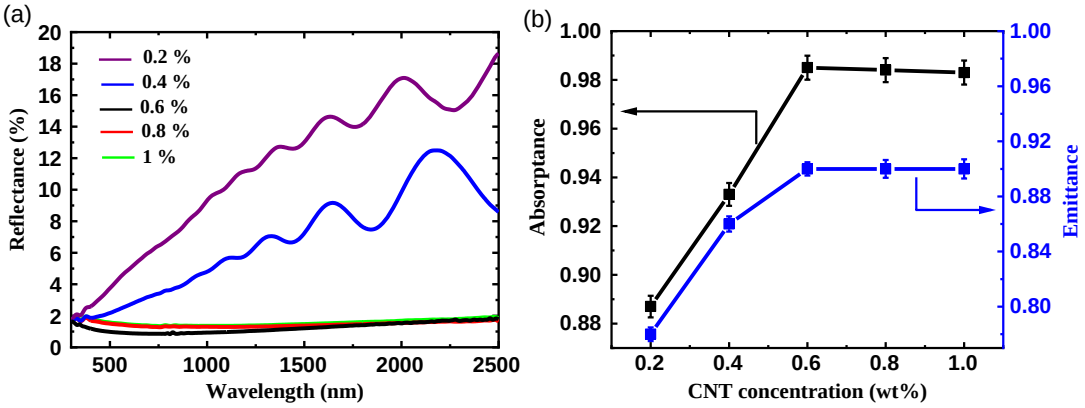

Figure 4. a) Reflectance spectra and b) absorptance of CNT@matrix prepared with various CNT concentration in the coating formulations.

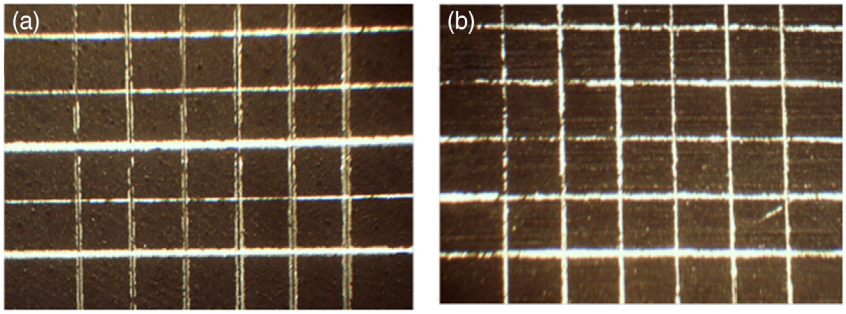

Figure 5. Images of the CNT@matrix coating after adhesion tests: a) ISO 2409 and b) ASTM D3359 standards.

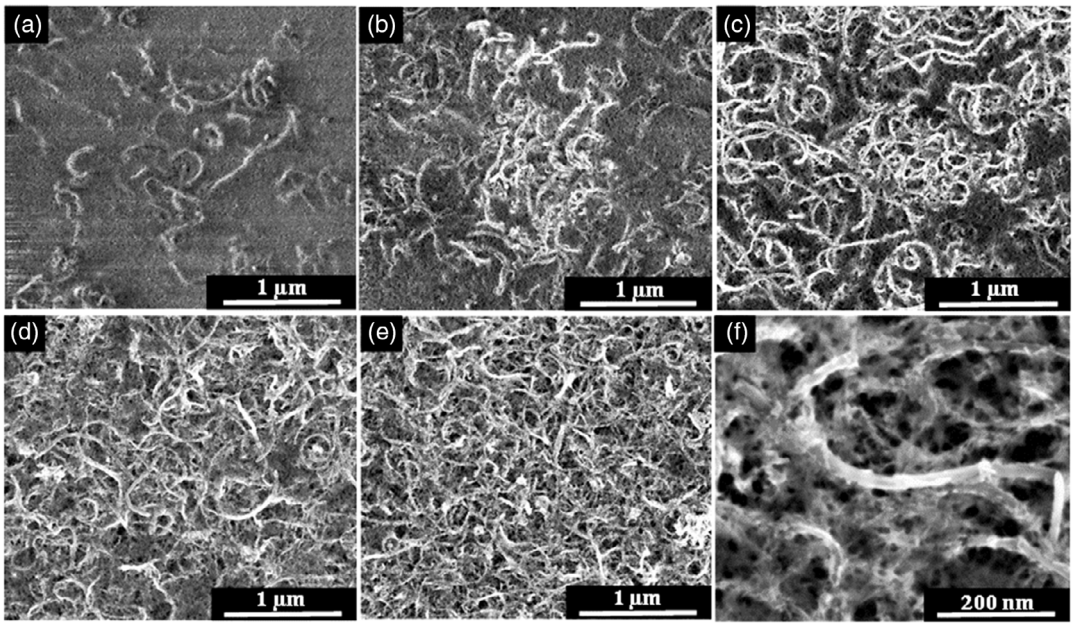

Figure 6. SEM images of CNT@matrix coatings with various CNT concentrations: a) 0.2%, b) 0.4%, c) 0.6%, d) 0.8%, and e) 1%. f) Shows the magnified image of CNT@matrix with 6% of CNT.

property of the coating, water was sprayed on both the as-prepared and oxygen plasma-treated CNT coatings. As shown in Figure S5, Supporting Information, although droplets were formed on the nontreated surface, the water was completely spread out on the treated CNT coating. Here, the effect of plasma treatment on the absorptance cannot be ruled out as it can decrease the absorptance. However, our study revealed that after plasma treatment, the calculated absorptance from the

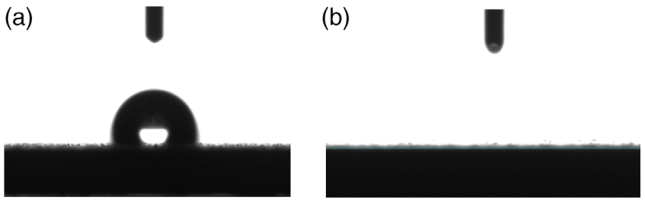

Figure 7. Wetting by individual water droplets of a) as-prepared and b) plasma-treated CNT@matrix coating.

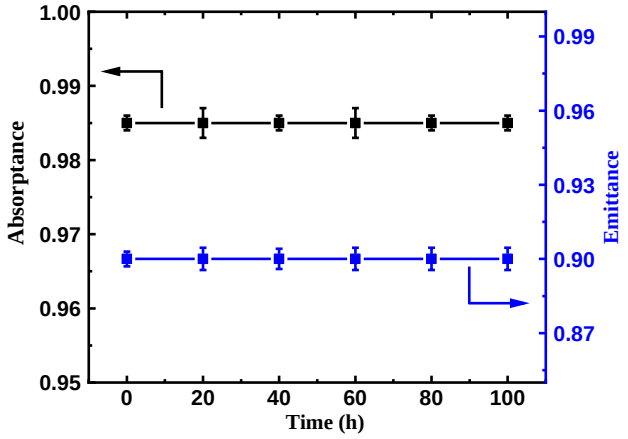

Figure 8. Absorptance of CNT@matrix coating with 0.6% of CNT at different duration at 350 °C.

reflectance spectra was the same as in the case of as-prepared CNT coating (Figure S6, Supporting Information). The generated oxygen functionalities only increase the wettability of the surface without affecting the absorptance.

The thermo-solar absorbers are expected to operate at high temperatures. Hence, we evaluated the CNT@matrix heat stability in air. The coatings were heated to 350 °C in air for various durations (**Figure 8**) and the absorptance of the coatings was measured after being cooled down to room temperature. It is evident that the coating is stable at 350 °C for at least 100 h.

To evaluate the efficiency of the developed coating, the selective absorber efficiency was calculated and compared to the reported selective W–Ni–Al_2O_3 cermet[30] and CNT/ITO inverse tandem[23] coatings as both the coatings have high selectivity (Table 1) with high absorptance ($\alpha = 0.9$ for W–Ni–Al_2O_3 and $\alpha = 0.938$ for CNT/ITO) and low emittance ($\varepsilon = 0.150$ for W–Ni–Al_2O_3 and $\varepsilon = 0.270$ for CNT/ITO). The selective efficiency of the absorbers as a function of solar concentration ratio at 100 and 250 °C is shown in **Figure 9**. From this study, it is observed that the CNT@matrix coating shows a higher absorber efficiency than the selective W–Ni–Al_2O_3 cermet and CNT/ITO inverse tandem coatings at low temperatures for concentration ratios higher than 45. Because of the relatively high thermal emittance of the CNT@matrix coating, its absorber efficiency is strongly reduced for higher temperatures, especially at low concentration ratios. Based on efficiency considerations, the best operation scenario of the analyzed CNT@matrix coating would be at low temperature and high concentration ratio applications. It is worth mentioning here that the near-perfect absorber with $\alpha/\varepsilon = 1$ may not have the same efficiency as in the present case ($\alpha/\varepsilon > 1$, $\alpha = 0.985$, and $\varepsilon = 0.901$) as the emittance has also been considered in evaluating the efficiency of the absorber.

4. Conclusion

In conclusion, we demonstrated a simple method for the fabrication of CNT-based near-perfect solar absorber by spraying at room temperature. The coating exhibited very high absorptance, 0.985. The coating showed durable self-cleaning properties upon oxygen plasma posttreatment. The coating had very good adhesion and showed high thermal stability without any change in the absorptance even after 100 h at 350 °C. Analytical models reveal that the CNT@matrix coating shows higher efficiency at low temperatures and at a high concentration ratio than that of previously reported selective coatings. We expect that the developed sprayable approach will open new possibilities for fabricating low-cost, self-cleaning, and highly efficient solar-thermal devices with large areas and curved surfaces such as tubes (Figure 1).

Supporting Information

Supporting Information is available from the Wiley Online Library or from the author.

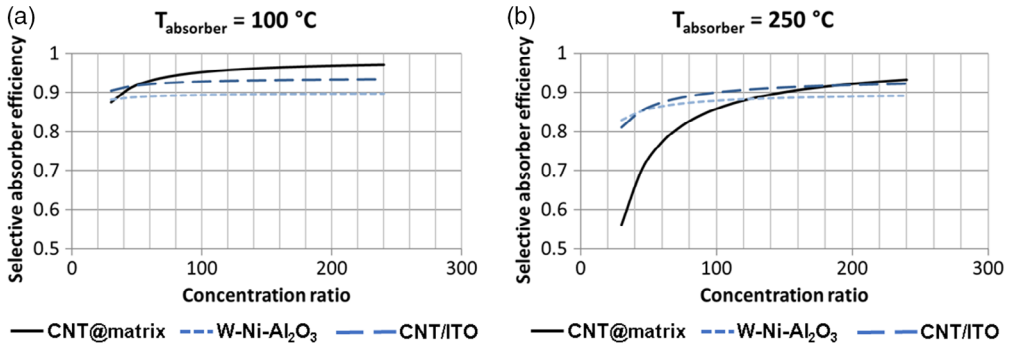

Figure 9. The efficiency of the absorbers as a function of solar concentration ratio at a) 100 °C and b) 250 °C with CNT, CNT/ITO, and W–Ni–Al_2O_3 cermet absorbers.

Acknowledgements

This work was financially supported by the Israel Ministry of Energy (217-11-043) and the Israel-Strategic Alternative Energy Foundation (ISAEF).

Conflict of Interest

The authors declare no conflict of interest.

Keywords

absorptance, carbon nanotubes, concentrated solar power, solar absorber coatings, solar-thermal coatings

Received: August 1, 2020
Revised: October 3, 2020
Published online:

[1] K. Mizuno, J. Ishii, H. Kishida, Y. Hayamizu, S. Yasuda, D. N. Futaba, M. Yumura, K. Hata, *PNAS* **2009**, *106*, 6044.
[2] H. Shi, J. G. Ok, H. W. Baac, L. J. Guo, *Appl. Phys. Lett.* **2011**, *99*, 211103.
[3] X. J. Wang, L. P. Wang, O. S. Adewuyi, B. A. Cola, Z. M. Zhang, *Appl. Phys. Lett.* **2010**, *97*, 163116.
[4] Z. P. Yang, L. Ci, J. A. Bur, S. Y. Lin, P. M. Ajayan, *Nano Lett.* **2008**, *8*, 446.
[5] N. Selvakumar, S. B. Krupanidhi, H. C. Barshilia, *Adv. Mater.* **2014**, *26*, 2552.
[6] P. Yu, H. Yang, X. Chen, Z. Yi, W. Yao, J. Chen, Y. Yi, P. Wu, *Renew. Energy* **2020**, *158*, 227.
[7] F. Qin, X. Chen, Z. Yi, W. Yao, H. Yang, Y. Tang, Y. Yi, H. Li, Y. Yi, *Sol. Energy Mater. Sol. Cells* **2020**, *211*, 110535.
[8] J. Li, X. Chen, Z. Yi, H. Yang, Y. Tang, Y. Yi, W. Yao, J. Wang, Y. Yi, *Mater. Today Energy* **2020**, *16*, 100390.
[9] J. Li, Z. Chen, H. Yang, Z. Yi, X. Chen, W. Yao, T. Duan, P. Wu, G. Li, Y. Yi, *Nanomaterials* **2020**, *10*, 257.
[10] A. Cao, X. Zhang, C. Xu, B. Wei, D. Wu, *Sol. Energy Mater. Sol. Cells* **2002**, *70*, 481.
[11] A. B. Kaul, J. B. Coles, M. Eastwood, R. O. Green, P. R. Bandaru, *Small* **2013**, *9*, 1058.
[12] J.-Q. Xi, M. F. Schubert, J. K. Kim, E. F. Schubert, M. Chen, S.-Y. Lin, W. Liu, J. A. Smart, *Nat. Photonics* **2007**, *1*, 176.
[13] M. J. Persky, *Rev. Sci. Instrum.* **1999**, *70*, 2193.
[14] F. Zhao, X. Chen, Z. Yi, F. Qin, Y. Tang, W. Yao, Z. Zhou, Y. Yi, *Sol. Energy* **2020**, *204*, 635.
[15] H. G. Craighead, R. E. Howard, J. E. Sweeney, R. A. Buhrman, *Appl. Phys. Lett.* **1981**, *39*, 29.
[16] R. K. Bera, Y. Binyamin, S. G. Mhaisalkar, S. Magdassi, D. Mandler, *Sol. RRL* **2017**, *1*, 1700080.
[17] NASA Develops Super-Black Material That Absorbs Light Across Multiple Wavelength Bands, https://www.nasa.gov/topics/technology/features/super-black-material.html (accessed: June 2020).
[18] M. E. Rincon, J. D. Molina, M. Sanchez, C. Arancibia, E. Garcia, *Sol. Energy Mater. Sol. Cells* **2007**, *91*, 1421.
[19] K. Roro, N. Tile, B. Mwakikunga, B. Yalisi, A. Forbes, *Mater. Sci. Eng. B* **2012**, *177*, 581.
[20] F. S. Schultz, *US 2009/0314284*, **2009**.
[21] M. Kurzböck, G. M. Wallner, R. W. Lang, *Energy Procedia* **2012**, *30*, 438.
[22] S. Azoubel, R. Cohen, S. Magdassi, *Surf. Coat. Technol.* **2015**, *22*, 21.
[23] R. K. Bera, S. Azoubel, S. G. Mhaisalkar, S. Magdassi, D. Mandler, *Energy. Technol.* **2015**, *3*, 1045.
[24] R. K. Bera, S. G. Mhaisalkar, D. Mandler, S. Magdassi, *Energy Convers. Manage.* **2016**, *120*, 287.
[25] R. Wang, K. Hashimoto, A. Fujishima, M. Chikuni, E. Kojima, A. Kitamura, M. Shimohigoshi, T. Watanabe, *Nature* **1997**, *388*, 431.
[26] F. C. Cebeci, Z. Z. Wu, L. Zhai, R. E. Cohen, M. F. Rubner, *Langmuir* **2006**, *22*, 2856.
[27] H. Liu, J. Zhai, L. Jiang, *Soft Matter* **2006**, *2*, 811.
[28] P. Li, X. Lim, Y. Zhu, T. Yu, C.-K. Ong, Z. Shen, A. T.-S. Wee, C.-H. Sow, *J. Phys. Chem. B* **2007**, *111*, 1672.
[29] H. Kinoshita, A. Ogasahara, Y. Fukuda, N. Ohmae, *Carbon* **2010**, *48*, 4403.
[30] F. Cao, D. Kraemer, T. Sun, Y. Lan, G. Chen, Z. Ren, *Adv. Energy Mater.* **2015**, *5*, 1401042.
[31] C. Ho, J. Pacheco, *Levelized Cost of Coating (LCOC) for Selective Absorber Materials*, Sandia National laboratories, Albuquerque, USA **2013**.
[32] C. A. Milea, E. Ienei, C. Bogatu, A. Duta, *J. Sol-Gel Sci. Technol.* **2013**, *67*, 112.
[33] R. Kirilov, P. Stefchev, Z. Alexieva, H. Dikov, *Solid State Phenomena* **2010**, *159*, 97.
[34] Test Methods for Adhesion Evaluation of Paints and Coatings, https://instruments.byk.com/fileadmin/byk/support/instruments/technical_information/datasheets/English/Physical%20Test/Adhesion/Test_Methods_for_Adhesion_Evaluation_of_Paints_and_Coatings.pdf (accessed: October 2020).